



# Demethylase FTO enhances the PI3K/Akt signaling to promote gastric cancer malignancy

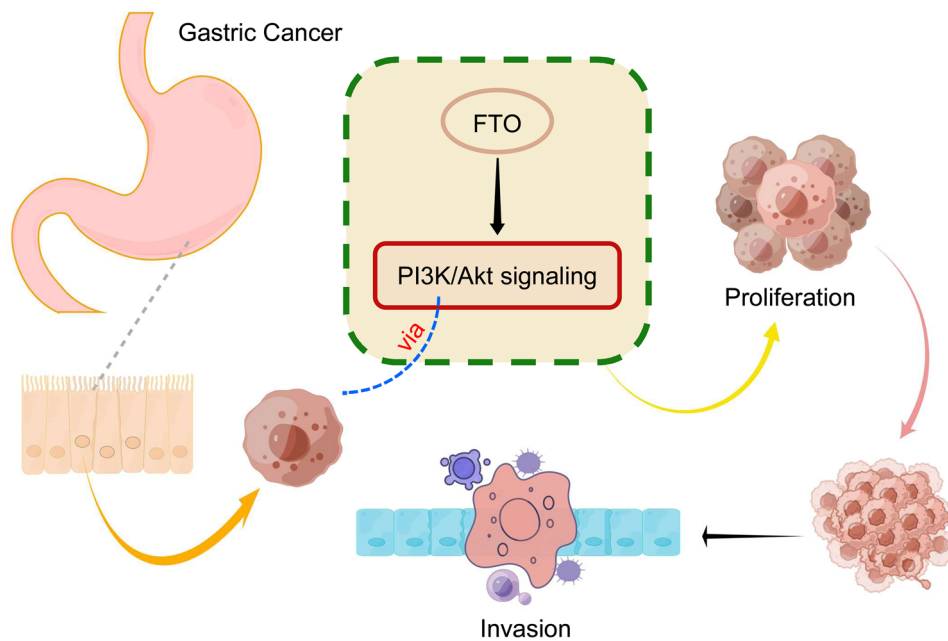
Yuxuan Zhu<sup>1</sup> · Jing Yang<sup>2</sup> · Yongxiang Li<sup>2</sup> · Jiegou Xu<sup>3</sup> · Zheng Fang<sup>1,2</sup>

Received: 29 January 2023 / Accepted: 6 March 2023 / Published online: 27 March 2023  
© The Author(s), under exclusive licence to Springer Science+Business Media, LLC, part of Springer Nature 2023

## Abstract

Enhanced expression of fat mass and obesity-associated protein (FTO) has been reported in gastric cancer (GC). Bioinformatical studies indicate that FTO expression is correlated with the patients' overall survival (OS). How FTO exerts its promotion effects on GC development and affects OS remains largely unknown. In this study, the prognostic relevance of FTO expression in human GC tissues and the molecular mechanisms underlying FTO's promotion roles were investigated. Kaplan–Meier survival curve analysis revealed that the patients with high FTO levels had shorter OS compared to those with low FTO expression ( $p < 0.0001$ ). Univariate and multivariate COX regression analyses showed that the patients' OS was affected by FTO status ( $p < 0.0001$ ,  $p = 0.001$ , respectively). FTO knockdown in HGC27 cells by shRNAs reduced cell proliferation, colony formation, migration and invasion, while FTO overexpression in AGS cells had reverse effects. FTO knockdown in HGC27 cells also suppressed the tumor growth in a mouse xenograft model. High-throughput transcriptome sequencing indicated that FTO enhanced the PI3K/Akt signaling, which was confirmed in vitro. In summary, our research revealed that FTO is a potent prognostic biomarker of GC. FTO enhances the PI3K/Akt signaling and thus, promotes GC development.

## Graphical Abstract



**Keywords** FTO · Gastric cancer · PI3K/Akt signaling pathway · Proliferation and metastasis · Prognosis

Extended author information available on the last page of the article

## Abbreviations

CI	Confidence interval
EMT	Epithelial-mesenchymal transition
FTO	Fat mass and obesity-associated protein
GC	Gastric cancer
HR	Hazard ratio
IHC	Immunohistochemistry
m6A	N6-methyladenosine
OS	Overall survival
SD	Standard deviation
TCGA	The Cancer Genome Atlas
TNM	Tumor node metastasis

## Introduction

Gastric cancer is among the most common malignancies. It has been reported to exceed 1 million new cases and cause 783,000 deaths worldwide, ranking the fifth highest incidence rate and the third highest mortality in 2018 [1]. In China, 679,100 new cases of gastric cancer in 2015 have been estimated, with 498,000 deaths, ranking the second to lung cancer [2]. Despite continuous progresses in the comprehensive treatment, the 5-year survival rate of advanced gastric cancer is still only 39.3–44.8% [3, 4]. Thus, intensive understanding of molecular mechanisms that affect prognosis of gastric cancer is necessary to find out key molecules in the pathogenesis of gastric cancer for therapeutic options.

RNA methylation is an important modification that regulate RNA translation and degradation at the post-transcriptional level and associated with many physiological and pathological processes. N6-methyladenosine (m6A), the most common endogenous RNA modification, is regulated by three types of key enzymes, i.e., writers, erasers and readers, which are able to write, erase and read the methyl groups in mRNA molecules, respectively [5–7]. Abnormal m6A modification in tumor-related functional genes-transcribed mRNA are frequently found in many tumors such as acute granulocytic leukemia, lung cancer, liver cancer, glioma, endometrial cancer and other tumors. Distorted regulation of the key enzymes will lead to enhanced expression of oncoproteins or accelerated degradation of tumor suppressors and ultimately affects the development of tumors [8–12]. In the brain glioma stem cells, silencing the RNA methyltransferase METTL3 or METTL14 upregulates expression of the oncogenes ADAM19, EPHA3 and KLF4, and simultaneously downregulates expression of the tumor suppressor genes CDKN2A, BRCA2 and TP53, promoting growth, self-renewal and tumorigenicity of cancer stem cells. On the contrary, overexpression of METTL3 inhibits the growth and colony formation of cancer stem cell [13]. Therefore, the m6A modification of tumor-related genes' mRNAs play an important role in tumor development.

Fat mass and obesity-associated protein (FTO) is the first identified RNA demethylase that can erase m6A modification. Deletion of m6A modification by FTO causes alternative splicing in the FTO-targeted mRNAs [14]. In tumorigenesis, FTO targets different genes and promote tumor cell growth in different cancers. FTO-regulated expression of ASB2 and RARA in acute myeloid leukemia enhances cell transformation and leukemogenesis [15], while  $\beta$ -catenin is up-regulated by highly expressed FTO in cervical squamous cell carcinoma, leading to resistance of the tumor cells to chemo-radiotherapy [16]. Increased expression of FTO in lung squamous cell cancer cells can enhance MZF1 expression by decreasing the m6A level in the MZF1 mRNA transcript to facilitate malignant phenotypes of the cells [17]. It is likely that FTO promotes cancer development through different pathways by targeting different molecules in the different cellular context.

Aberrant m6A methylation and enhanced FTO expression in gastric cancer have been reported in several studies [18, 19]. Increased FTO expression promotes cell proliferation and malignant phenotypes of gastric cancer cells by targeting different genes [18, 20, 21]. Although bioinformatical analyses indicate that FTO is a potential prognostic biomarker [22–24], actual clinical evidence is still lacking. In this study, we focused on prognostic value of FTO expression in human gastric cancer tissues and the signaling pathways involved in FTO-induced malignant phenotypes.

## Material and methods

### Cell lines and cell culture

Human gastric cancer cell lines (AGS, SNU-1, HGC27 and NCI-N87) and the human fibroblast cell line HEK293T were purchased from Procell (Wuhan, China). AGS cells and the other gastric cancer cells were cultured in DMEM/F-12K (Bio-Channel, China) and RPMI-1640 (Bio-Channel, China) media supplemented with 10% fetal bovine serum (FBS, Gibco BRL, USA), respectively, while HEK293T cells were maintained in 10% FBS DMEM (Bio-Channel, China).

### Gastric cancer tissue chip and Immunohistochemistry

A tissue chip containing 107 gastric cancer tissues and 20 adjacent normal tissues was obtained from Department of General Surgery, the First affiliated Hospital of Anhui Medical University. All the patients' death dates were documented and overall survival (OS) was calculated as the time from the surgical operation date to the date of death.

Immunohistochemistry (IHC) analysis of FTO was performed using an IHC kit (9710, Maixin, China). Briefly, the

chip was baked at 60 °C for an hour, dewaxed in xylene, and rehydrated in decreasing concentrations of ethanol as quidded by the manufacturer. After treated with endogenous catalase blocking and subsequent nonspecific blocking, the chip was incubated with 1:500 diluted FTO antibody (ab126605, Abcam) overnight. After washing, the slide was incubated with anti-rabbit secondary antibodies conjugated with streptomyces biotin-horseradish peroxidase for 30 min. DAB detection kit (DAB-G1212, Servicebio, China) was used for the chromogenic reaction and hematoxylin was used for counterstaining, and finally, the slide was mounted with neutral resin.

The immunohistochemistry staining was examined double-blindly by two independent pathologists. Based on the intensity of FTO staining, categories and scoring of FTO expression were created as following: negative, less than 5% positive tumor cells, 0 point; weak, 5–25% positive tumor cells, 1 point; medium, 25–50% positive tumor cells, 2 points; strong, 50–75% positive tumor cells, 3 points; very strong, 75% positive tumor cells, 4 points.

### Tissue specimens of human gastric cancer

Surgically resected ten pairs of gastric tissue specimens (tumor and adjacent mucosa) were collected from patients hospitalized in the First Affiliated Hospital of Anhui Medical University and immediately frozen in liquid nitrogen for qPCR and western blotting analyses of FTO expression. Informed consent was obtained from each patient.

### Western blotting assay

Cultured cells or tissues were lysed in RIPA lysis buffer (Beyotime, China). After centrifugation, total protein in the supernatants was determined by the Bradford method. Aliquots of the supernatants containing 20 µg protein were separated in 10% SDS-PAGE and then transferred onto Millipore PVDF membranes. The membranes were blocked for 2 h in 5% nonfat milk and incubated overnight at 4 °C with diluted primary antibodies: anti-FTO (1:1000), anti-Vimentin (1:1000), anti-E-cadherin (1:5000), anti-N-cadherin (1:2000), anti-Akt (1:1000), anti-p-Akt (1:2000), anti-PI3K (1:500), anti-p-PI3K (1:1000), and anti-GAPDH (1:5000). The anti-p-PI3K was obtained from Cell Signaling Technology and the other antibodies were purchased from ProteinTech. The HRP-labeled secondary goat anti-rabbit IgG (1:10,000, ProteinTech) was applied to membranes for 2 h at room temperature. After washing three times with TBST, the signals were detected with a chemiluminescence detection system (Thermo Scientific, USA). GAPDH was used as an internal control, and image J V2 software was used to measure signal densities.

### Reverse transcription and quantitative PCR (RT-qPCR)

The total RNA was extracted from cells and tissues using TRIzol<sup>®</sup> reagent (Invitrogen, Thermo Fisher Scientific, USA) and 1 g of total RNA were reverse-transcribed with HiScript Q RT SuperMix (Vazyme Biotech, China). qPCR was performed using AceQ qPCR SYBR Green Master Mix (Vazyme Biotech) with the following cycling parameters: 40 cycles of 95 °C for 10 s and 60 °C for 30 s, followed by 95 °C for 5 min. Relative expression of each gene was calculated using  $2^{-\Delta\Delta Cq}$  method and GAPDH expression was used as an internal normalization control. The gene-specific primers are indicated in Table S1.

### Knockdown and overexpression of FTO in gastric cancer cells

The lentiviral vector pCLenti-U6-shRNA-CMV-Puro-WPRE (OBiO Technology, China) was used for construction of shRNA expression vectors. The expression of shRNAs was under control of the U6 promoter using puromycin for selection. Two shRNA sequences targeting FTO, designated as shFTO#1 and shFTO#2, are listed in the Table S1. For overexpression of FTO, the human FTO gene (NM-0010804323) was inserted into the Xho1-Not1 site of the lentiviral vector pLvX (GENEWIZ, China). To produce viral preparations, Lipofectamine 2000 (Invitrogen, USA) was used to transfect HEK293T cells with the knockdown or overexpression lentiviral vectors and the packaging plasmids PsPax and PMD2G (GENEWIZ). After transfection, viral supernatants were collected 48 to 72 h later and added to gastric cancer cells treated with polybrene at 10 mg/ml. After puromycin selection at 2 mg/ml for seven days, the cells were maintained with puromycin until use.

### Cell viability assay

3000 cells per well were seeded into 96-well plates and cultured in fresh 10% FBS RPMI-1640 medium for 24 h, 48 h, 72 h, or 96 h. The cell viability was determined by adding 10 µl of Cell Counting Kit-8 (CCK-8, TargetMol, China) and measuring absorbance at 450 nm.

### Colony formation assay

1500 gastric cancer cells were plated in each well of a 6-well dish and incubated for two weeks until the cell colonies were visible. After washing with PBS and fixation in 4% paraformaldehyde for 20 min, the cells were

stained with 0.1% crystal violet for 15 min. The colonies containing at least 50 cells observed under microscope were counted.

### Wound healing assay

GC cells were seeded into a 6-well plate at a density of  $1 \times 10^5/\text{cm}^2$ . After the cell grew to a monolayer, a wound space in the center was made by scratching the attached cells using a pipette tip. The cells were washed with PBS thrice to rinse off the detached cells. Then, 2 ml of RPMI-1640 (Bio-Channel) containing 2%FBS (Gibco) was added, the wounds were photographed under a microscope (CKX53, Olympus, Japan) at 0 and 24 h, and the scratch widths were measured.

### Transwell invasion assay

The invasion assay was performed with the Transwell Invasion Kit (Corning Incorporation, USA). Briefly, the transwell inserts were added with matrix gel 1:10 diluted in serum-free RPMI-1640 medium and incubated at 37 °C for 24 h to allow the gel solidified, and then laid onto a 24 well plate which was added in advance with 700 ml of 10% FBS RPMI-1640 medium per well.  $3 \times 10^4$  cells in 200 ml serum-free RPMI-1640 medium were seeded into each insert and incubated at 37 °C for 48 h. After removal of the medium in the inserts, the cells on the downside surface of the inserts were fixed in 4% paraformaldehyde for 20 min and stained with 0.1% crystal violet for 15 min. Finally, five randomly selected sight fields under 20× microscopy were photographed and the cells were counted.

### Xenograft gastric cancer model

Athymic female mice (BALB/c nu/nu; 4 weeks old) were obtained from Huachuang Sino, were raised in a specific pathogen-free environment and provided with free access to food and water. After one-week acclimation, the mice were randomly divided in three groups each having 6 mice: control group, shFTO#1 group and shFTO#2 group. Each mouse of the three groups was implanted in the flank with  $4 \times 10^6$  control HGC27 cells, shFTO1-infected HGC27 cells or shFTO2-infected HGC27 cells. The tumor growth was monitored every three days and the tumor volumes were calculated using the formula of  $0.5 \times \text{length} \times \text{width}^2$ . 33 days after the implantation, all the mice were sacrificed, and the tumors were weighed and fixed in 4% paraformaldehyde for IHC analysis.

### High-throughput transcriptome sequencing

For high-throughput transcriptome sequencing, total RNA was extracted from the control and shFTO knockdown

HGC27 cells using Trizol reagent (Invitrogen, CA, USA). The isolated mRNA samples were subjected for custom service of GENEWIZ (Suzhou, China) with the Illumina Novaseq 6000. Differentially expressed genes were analyzed and signaling pathways were enriched.

### Statistical analysis

Statistical analyses were performed using GraphPad Prism 8.0 (GraphPad Inc., San Diego, California) and SPSS 20.0 (SPSS Inc., Chicago, IL, USA). The data were expressed as mean  $\pm$  standard deviation (SD). Student's *t* test or one-way ANOVA was used to compare two groups or multiple groups.  $p < 0.05$  was considered statistically significant.

## Results

### Enhanced FTO expression was positively associated with poor prognosis of gastric cancer patients

For investigation of the relationship between FTO expression and prognosis, a human tissue chip containing 107 gastric cancer tissues and 20 adjacent normal tissues was used for immunohistochemical evaluation of FTO expression (Fig. 1a). Enhanced FTO expression was found mainly in the nucleus of gastric cancer cells (Fig. 1b). FTO expression scoring for each specimen was made on the basis of its IHC intensity, and the patients were divided into low FTO expression ( $n=63$ ) and high FTO expression ( $n=44$ ) groups. Figure 1b showed the representative FTO staining images of the high and low groups. The clinicopathological features including age, sex, tumor differentiation, tumor size, tumor site, tumor depth, lymph node metastasis, TNM were summarized in Table S2. Analysis of the associations of these features with FTO expression status indicated that only lymph node metastasis was significantly correlated, with the *p* value of 0.0003, respectively (Table S2). Further exploration of the correlation of FTO expression status with the patients' OS using the Kaplan–Meier survival curve revealed that the patients with high FTO levels had shorter OS time compared to those with low FTO expression ( $p < 0.0001$ ), with a hazard ratio (HR) of 3.989 (Fig. 1c). Univariate COX regression analysis showed that the patients' OS was affected by lymph node metastasis ( $p=0.005$ ), TNM stage ( $p < 0.037$ ) and FTO status ( $p < 0.0001$ ), while multivariate COX regression analysis revealed that the FTO score was the only factor influencing the OS, with  $p=0.001$ , HR = 5.291 and 95% CI 1.893–14.78 (Table 1), indicating that high FTO expression in gastric cancer cells was a potent biomarker for poor prognosis of gastric cancer patients. Consistent with the results described above, a correlation of high FTO

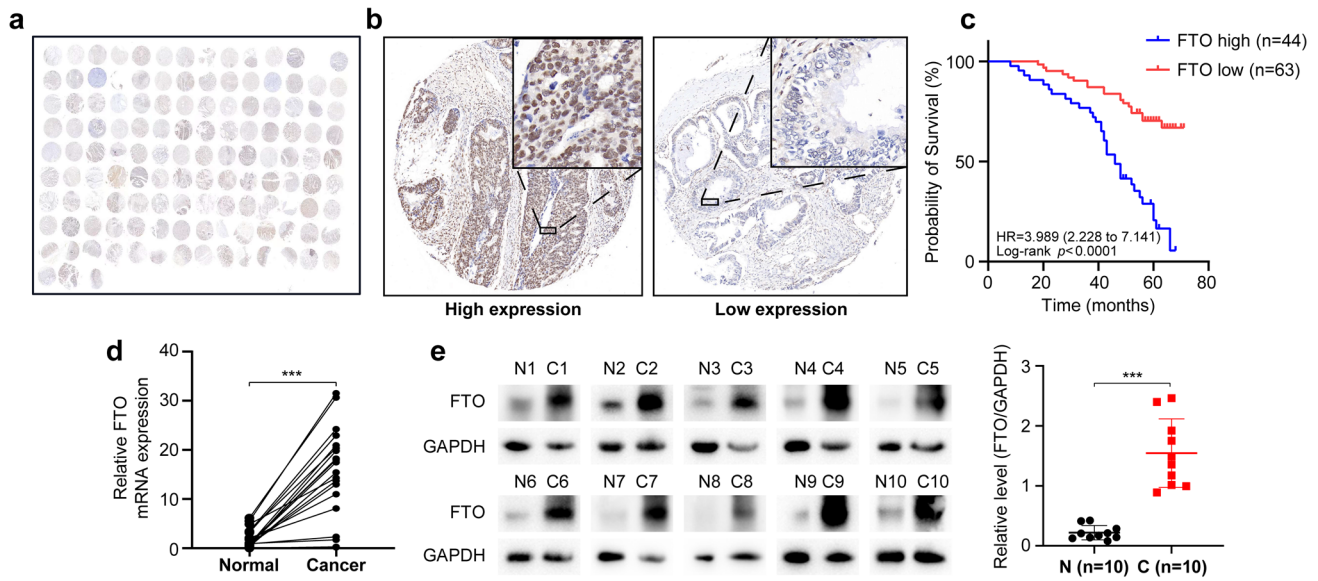


**Fig.1** FTO expression in gastric cancer tissues and its prognostic value

**Table 1** Univariate and multivariate cox regression analysis of prognostic factors in gastric cancer patients

Variables	OS univariate		OS multivariate	
	HR (95% CI)	<i>p</i> value	HR (95%CI)	<i>p</i> value
FTO status	4.057 (2.300–7.158)	<b>&lt;0.0001</b>	4.059 (2.131–7.729)	<b>&lt;0.0001</b>
Gender (male vs female)	0.912 (0.512–1.624)	0.753	1.303 (0.726–2.337)	0.977
Age (<61 vs ≥61)	1.271 (0.731–2.210)	0.395	1.303 (0.726–2.337)	0.375
Site (proximal vs distal)	1.157 (0.645–2.076)	0.624	0.826 (0.425–1.606)	0.573
Tumor size (<6 cm vs ≥6 cm)	0.677 (0.397–1.156)	0.153	0.576 (0.321–1.031)	0.063
Depth (1/2 vs 3/4)	1.589 (0.833–3.030)	0.160	1.614 (0.693–3.758)	0.267
Differentiation (1 vs 2)	1.659 (0.924–2.977)	0.090	1.164 (0.580–2.337)	0.669
Node (negative vs positive)	3.764 (1.494–9.487)	<b>0.005</b>	1.255 (0.352–4.476)	0.727
TNM Stage (T1–2 vs T3–4)	1.979 (1.041–3.763)	<b>0.037</b>	1.001 (0.408–2.458)	0.998

The *p* value in bold indicates that the *p* value is statistically significant (*p* value < 0.05)

CI confidence interval, HR hazard ratio, IHC immunohistochemistry, OS overall survival, TNM tumor node metastasis

expression with poor prognosis in gastric cancer patients was also concluded from the TCGA database (Fig.S1).

We further detected FTO expression in ten pairs of gastric cancer and adjacent tissues. As shown in Fig. 1d, qPCR analysis indicated that the mRNA expression was obviously higher in the gastric cancer tissues than in the adjacent tissues. Similarly, the protein levels in the cancer tissues detected by western blotting were significantly increased compared to those in the adjacent tissues (Fig. 1e).

A human gastric tissue chip containing 107 gastric cancer tissues and 20 adjacent tissues was used for IHC staining of FTO (a). Representative images of high and low FTO expression in the gastric cancer tissues from the tissue chip were shown (b). The association of FTO expression with the patients' overall survival was analyzed by the Kaplan–Meier

curve (c). FTO expression in 10 pairs of frozen gastric cancer tissues and the adjacent tissues was detected by qPCR (d) and western blotting, using GAPDH as an internal control (e). The SPSS 20.0 software was used for statistical analyses, and \*\*\* represents a *p* value less than 0.001.

### FTO promoted malignant phenotypes of gastric cancer cells in vitro

Examination of FTO expression in four gastric cancer cell lines by qPCR and western blotting revealed that, although FTO expression was detected in all the four gastric cancer cell lines, the expression levels were much higher in HGC27 and NCI-N87 cells than in AGS and SNU-1 cells (Fig. S2a, b). HGC27 cells and AGS cells were chosen to

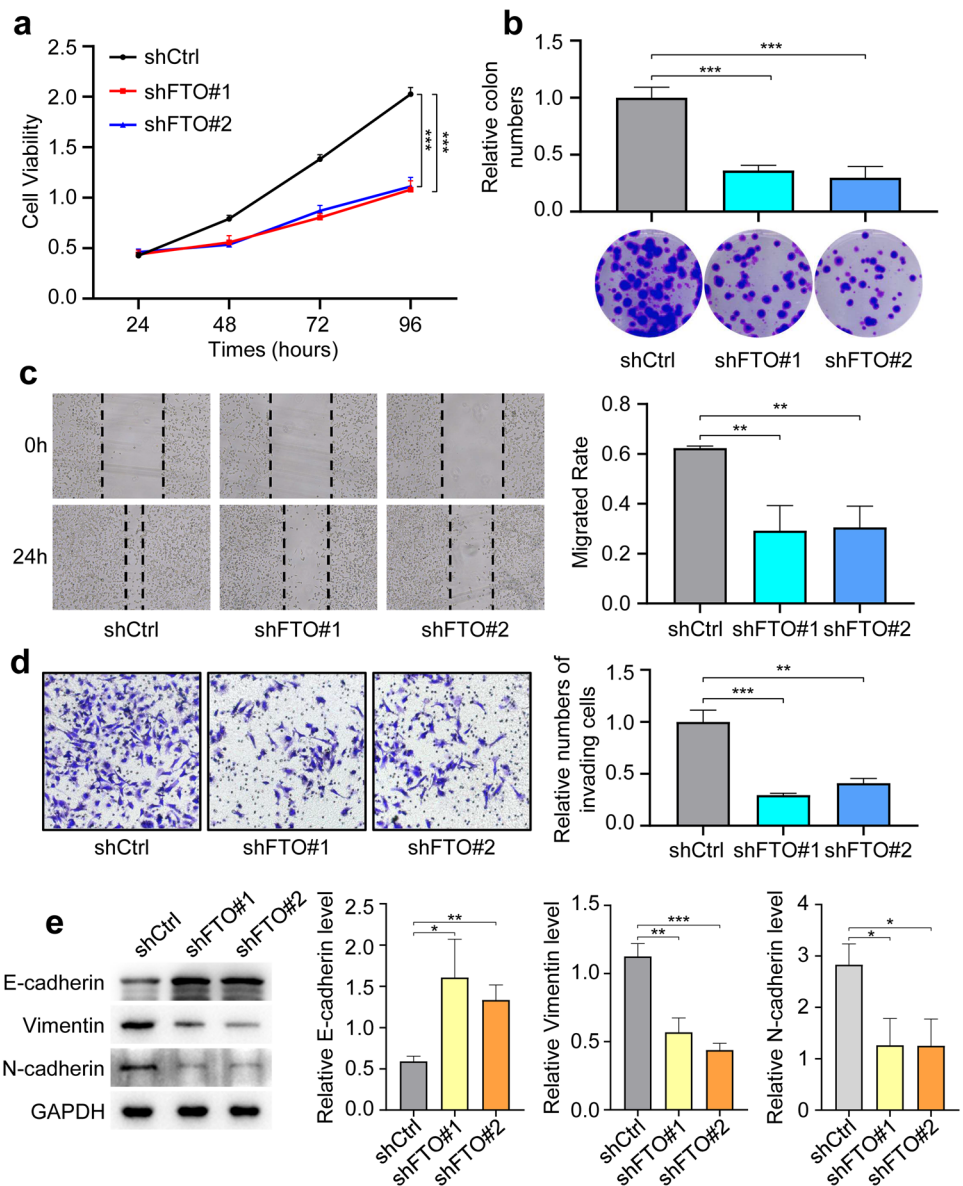


establish FTO knockdown or FTO-overexpressed cells for studying the impact of FTO expression on malignant phenotypes of gastric cancer cells. In the HGC27 cells infected with the lentiviruses expressing FTO shRNAs (shFTO#1 or shFTO#2), both FTO protein and mRNA expression were significantly knocked down as detected by western blotting and qPCR (Fig. S2c, d). Also, enhanced FTO protein and mRNA expression was observed in the AGS cells stably overexpressing FTO, compared with the cells infected with the vacant lentiviral vector (Fig. S2e, f).

The effects of FTO expression in gastric cancer cells on malignant phenotypes, including cell proliferation, colony formation, migration and invasion, were examined *in vitro*. Knockdown of FTO expression by shFTO#1 or shFTO#2 in HGC27 cells significantly reduced the cell proliferation

as compared with the irrelevant control RNA (Fig. 2a). Similarly, the colony number in the FTO-knocked down HGC27 cells was significantly fewer than that in the control cells (Fig. 2b), displaying that ability of colony formation was influenced by FTO expression. As shown in Fig. 2c, the wound healing assay revealed that FTO knockdown depressed the cell migration. Also, the invasion ability of HGC27 cells detected by Transwell assays was remarkably reduced by FTO knockdown (Fig. 2d). Western blotting detection and subsequent density determination showed that in the FTO-knocked down HGC27 cells, E-cadherin protein level were significantly increased, while vimentin and N-cadherin protein levels were significantly decreased (Fig. 2e), indicating that increased cell migration and invasion abilities in gastric cancer cells are probably due to

**Fig.2** The effects of FTO knockdown on malignant phenotypes of HGC27 cells



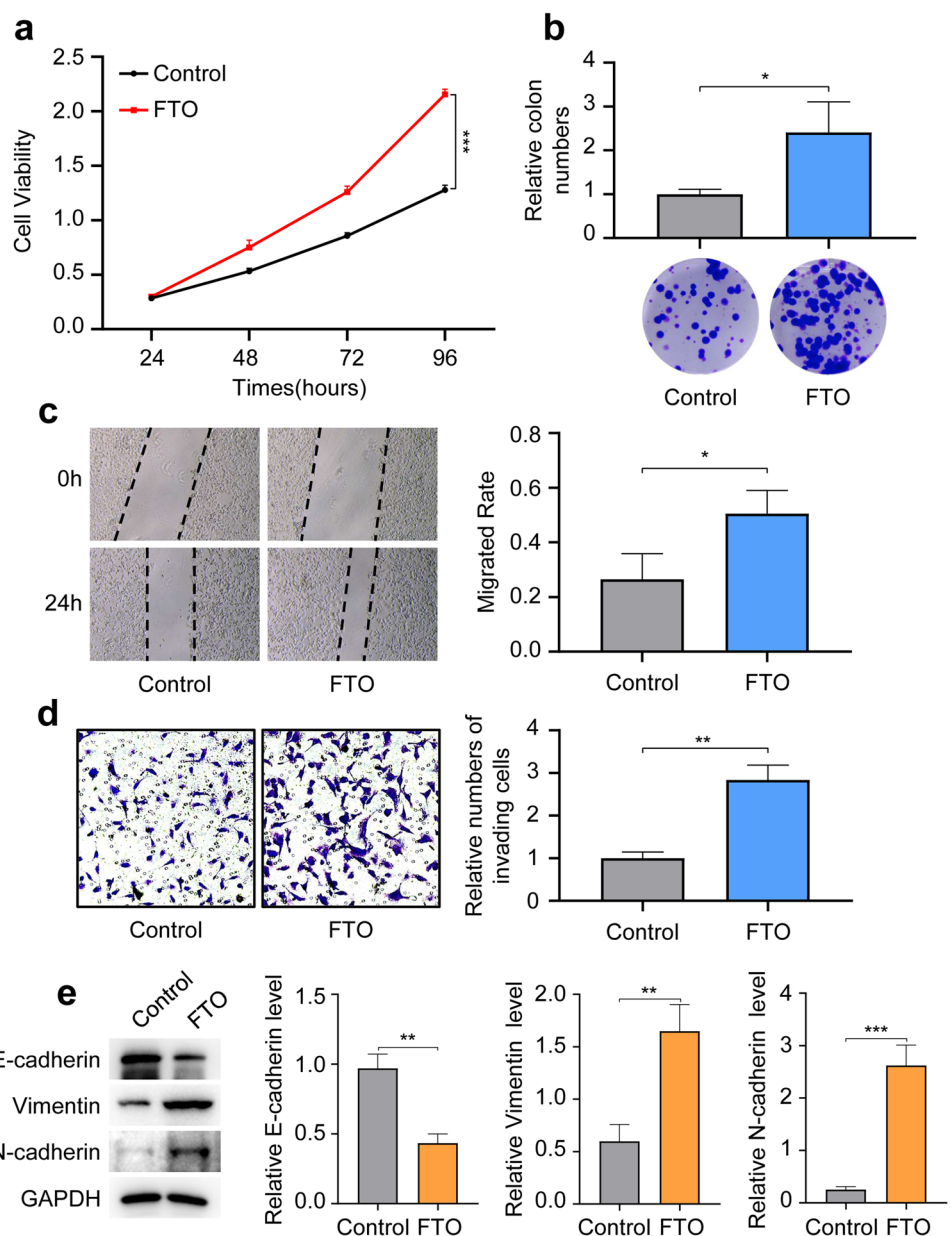
FTO-induced epithelial-mesenchymal transition (EMT). In contrast to the FTO-knocked down HGC27 cells, FTO overexpression in the AGS cells enhanced cell proliferation, colony formation, migration, invasion and EMT (Fig. 3).

Knockdown of FTO overexpression in HGC27 cells was performed using a lentiviral vector expressing shRNAs for human FTO. The cell proliferation (a), colony formation (b), migration (c) and invasion (d) were compared between the irrelevant RNA-expressing control vector (shCtrl) and the shRNA-expressing vector (shFTO#1 and shFTO#2) by Cell Counting Kit-8, dish colony formation, wound healing assay and Transwell invasion assay, respectively. E-cadherin, N-cadherin and vimentin, markers for epithelial-mesenchymal transition (EMT), were detected by western blotting and

quantified using Image J, with GAPDH as an internal control (e). Data from at least three independent experiments are expressed as mean  $\pm$  SD; The SPSS 20.0 software was used for statistical analyses. \*, \*\* and \*\*\* represent *p* values less than 0.05, 0.01 and 0.001, respectively.

FTO overexpression in AGS cells was performed using a lentiviral vector expressing human FTO. The cell proliferation (a), colony formation (b), migration (c) and invasion (d) were compared between the vacant control vector (control) and the expressing vector (FTO) by Cell Counting Kit-8, dish colony formation, wound healing assay and Transwell invasion assay, respectively. E-cadherin, N-cadherin and vimentin, markers for EMT, were detected by western blotting and quantified using Image J, and GAPDH was used as

**Fig.3** The effects of FTO overexpression in AGS cells on cell proliferation, colony formation, migration, invasion and EMT



an internal control (e). Data from at least three independent experiments are expressed as mean  $\pm$  SD; The SPSS 20.0 software was used for statistical analyses. \*, \*\* and \*\*\* represent  $p$  values less than 0.05, 0.01 and 0.001, respectively.

### Knockdown of FTO expression reduced tumor growth in a mouse xenograft model

For confirmation of the FTO promotion effect on gastric cancer growth in vivo, a xenograft model in nude mice was established, in which the HGC27 cells infected with the control, shFTO#1 or shFTO#2 viruses were implanted in the flank of the mice (Fig. 4a). Monitoring the tumor volume every 3 days revealed that knockdown FTO expression either by shFTO#1 or by shFTO#2 remarkably inhibited the tumor growth, as compared with the control group (Fig. 4b). As shown in Fig. 4c, d, the tumor size and weight were also decreased by both the shRNAs. Expectedly, IHC examination of the tumor tissues found that expressions of FTO and Ki67 (a marker for proliferative cells) were repressed by the shRNAs (Fig. 4e), and the level of E-cadherin was increased, while vimentin and N-cadherin expression levels were significantly decreased (Fig. S3).

BALB/c nude mice were implanted in the flank with HGC27 cells infected with the control, shFTO#1 or shFTO#2 lentiviruses and observed for 33 days (a). The growing tumor volume was monitored every 3 days (b). The

tumor size and weight at sacrifice are shown (c, d). Data are presented as means  $\pm$  sem. The SPSS 20.0 software was used for statistical analyses. \*, \*\* and \*\*\* represent  $p$  values less than 0.05, 0.01 and 0.001, respectively. Expression of FTO and Ki67 in the tumor tissues was examined by IHC. The scale bars, 100  $\mu$ m (e).

### The PI3K/Akt signaling pathway mediated FTO-induced promotion of gastric cancer

For understanding of the molecular mechanisms underlying the FTO-induced promotion roles in gastric cancer phenotypes, the HGC27 cells infected with the control viruses or the shRNA#1 were subjected for high-throughput transcriptome sequencing. A total of 20 differentially expressed genes were induced by FTO knockdown (Fig. 5a), with ten up-regulated and ten down-regulated (Fig. 5b). KEGG pathway analysis showed that the differentially expressed genes were significantly enriched in the PI3K/Akt pathway (Fig. 5c). As a result, Western blotting was used to detect the expression of the PI3K/Akt pathway-associated proteins in the manipulated gastric cancer cells. Knockdown of FTO in HGC27 cells by either shRNA#1 or shRNA#2 did not alter the protein levels of Akt and PI3K (Fig. 5d). However, phosphorylated Akt and PI3K were reduced by both shRNA#1 and shRNA#2 (Fig. 5d, e). Contrary to FTO knockdown in HGC27 cells, FTO overexpression in AGS cells increased

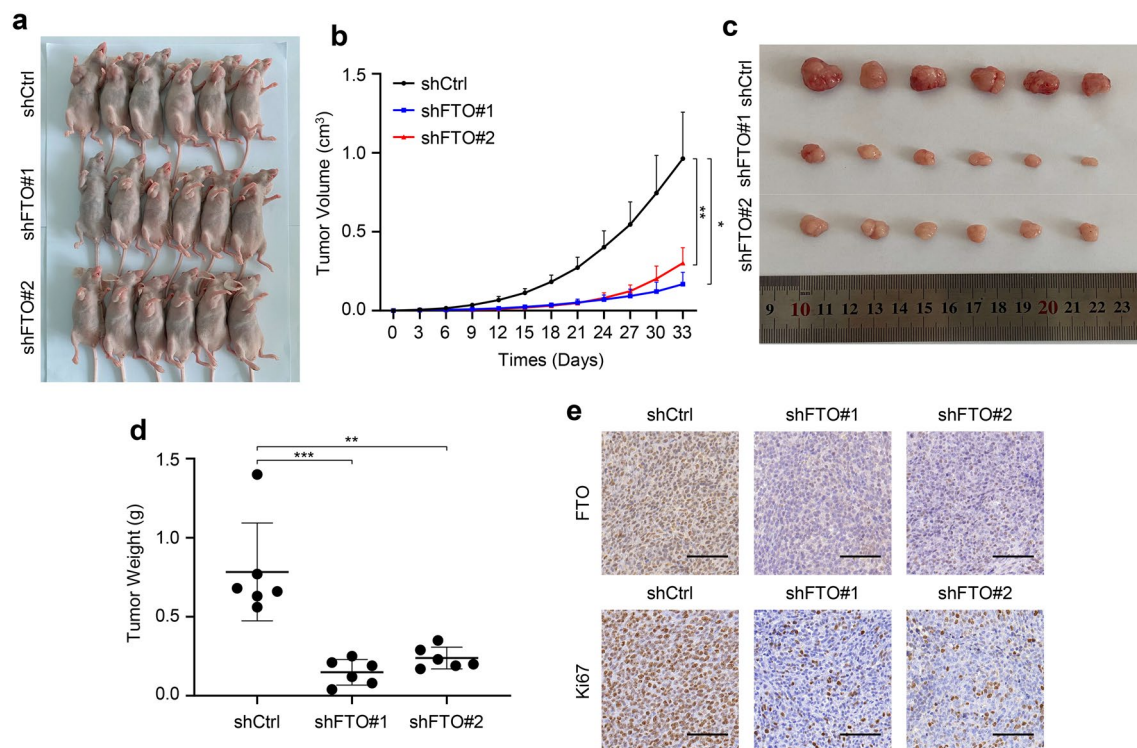


**Fig. 4** Inhibition of gastric cancer growth in mice by FTO knockdown



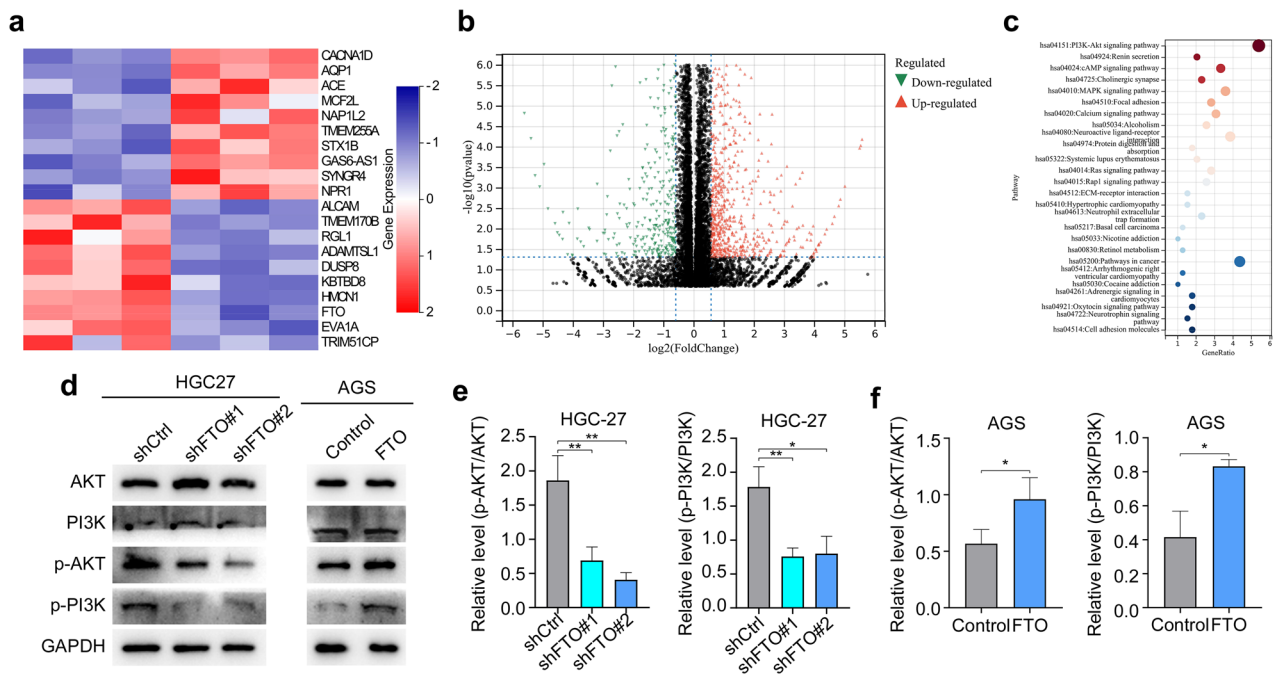


**Fig.5** High-throughput transcriptome sequencing and signaling pathway analysis

the phosphorylated Akt and PI3K, while the total amounts of Akt and PI3K remained unchanged (Fig. 5d, f). These results further confirmed that FTO enhanced the PI3K/Akt signaling in gastric cancer cells.

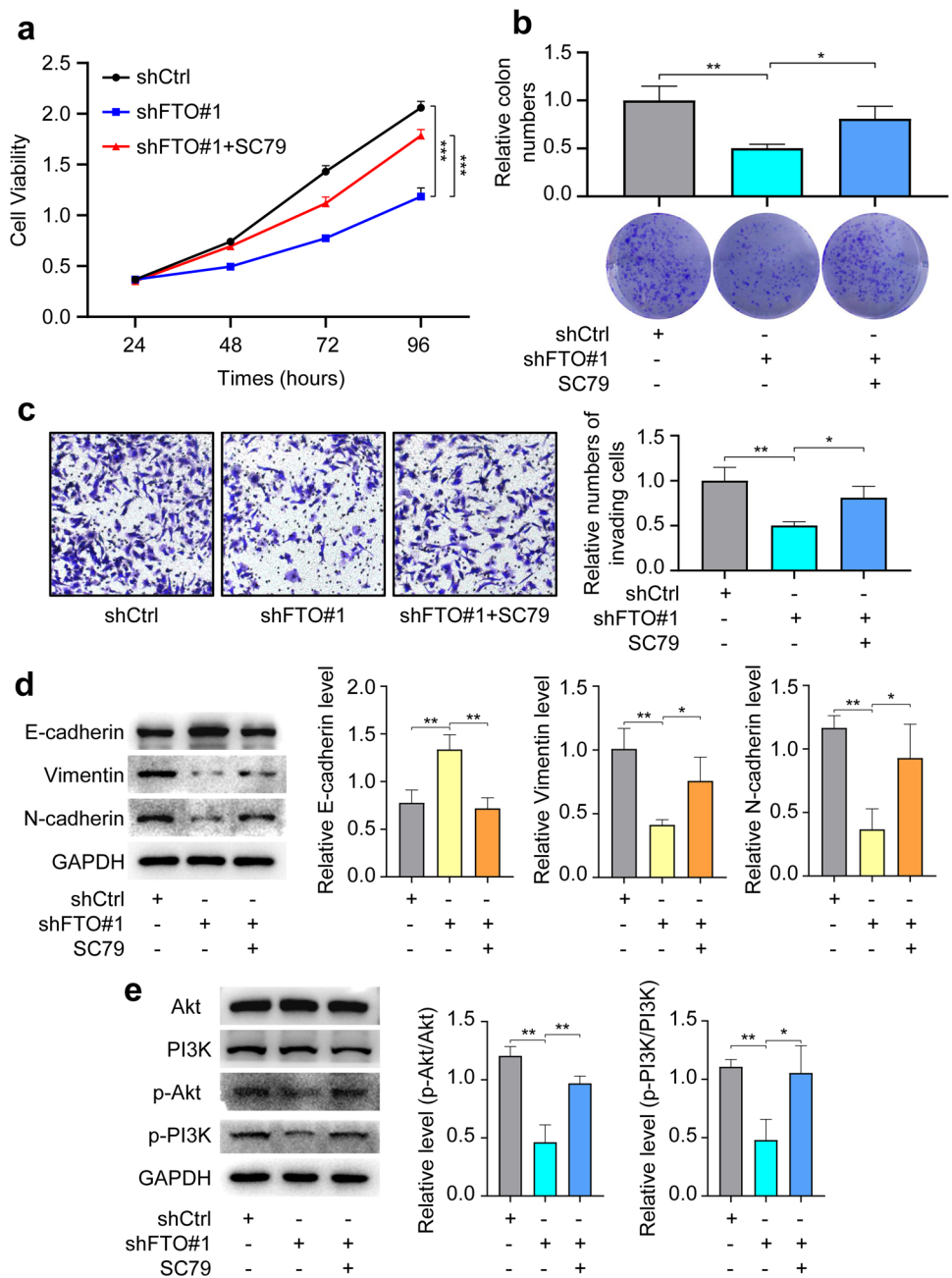
The HGC27 cells infected with the control lentiviruses or the shRNA#1 lentiviruses were subjected for high-throughput transcriptome sequencing. The heatmap and volcano plot of the differentially expressed genes are shown in (a, b). The altered signaling pathways were analyzed by the KEGG pathway enrichment analysis and the most relevant pathway was the PI3K/Akt signaling pathway (c). Phosphorylated PI3K and Akt in the FTO-knocked down HGC27 cells or FTO-overexpressed AGS cells were detected by western blotting (d) and their relative amounts were quantified with Image J (e, f). Data from at least three independent experiments are expressed as mean ± SD. The SPSS 20.0 software was used for statistical analyses. \* and \*\* represent *p* values less than 0.05 and 0.01, respectively.

SC79, a permeable Akt phosphorylation activator that is able to enhance the PI3K/Akt signaling, was used to observe whether FTO knockdown-induced inhibitory effects on the PI3K/Akt signaling and malignant phenotypes of gastric cancer can be rescued. As expected, shFTO#1 suppressed HGC27 cell proliferation. Addition of SC79 to shFTO#1-infected HGC27 cells largely restored the shFTO#1-induced suppressing effect on cell proliferation (Fig. 6a). Similarly, the decreases in the colony formation and cell invasion caused by shFTO#1 were

reversed by SC79 (Fig. 6b, c). The down-regulated vimentin and N-cadherin and up-regulated E-cadherin induced by shFTO#1 were partially inverted by the treatment of SC79 (Fig. 6d). Examination of phosphorylated PI3K and Akt by western blotting confirmed that the inhibited PI3K/Akt signaling caused by shFTO#1 was also recovered by SC79 (Fig. 6e). These results demonstrate that promotion effects of FTO on malignant phenotypes of gastric cancer cells are, at least partially, via the PI3K/Akt signaling pathway.

HGC27 cells were infected with the shRNA#1 lentiviruses to knockdown FTO and added with or without SC79, a PI3K/Akt pathway activator. The cell proliferation (a), colony formation (b), and invasion (c) were compared between the irrelevant RNA-expressing control lentivirus (shCtrl), the shRNA-expressing lentivirus (shFTO#1), and shFTO#1 plus SC79 by Cell Counting Kit-8, dish colony formation, and Transwell invasion assay, respectively. E-cadherin, N-cadherin and vimentin, markers for EMT, were detected by western blotting and quantified using Image J, with GAPDH as an internal control (d). Phosphorylated PI3K and Akt were detected by western blotting and their relative amounts were quantified with Image J (e). Data from at least three independent experiments are expressed as mean ± SD. The SPSS 20.0 software was used for statistical analyses. \*, \*\* and \*\*\* represent *p* values less than 0.05, 0.01 and 0.001, respectively.

**Fig.6** Involvement of FTO-enhanced PI3K/Akt signaling in the malignant phenotypes



## Discussion

It has been reported that enhanced FTO expression promotes tumor malignancy in several cancers [25, 26]. FTO expression is also up-regulated in gastric cancer and promotes cell proliferation and metastasis [18, 19]. Bioinformatic analyses reveal that up-regulated FTO is associated with poor prognosis in gastric cancer [21]. In the current study, we addressed two questions: (1) FTO expression in gastric cancer tissues and its association with the patients' prognosis; and (2) the molecular mechanisms underlying enhanced FTO expression in gastric cancer. By using a tissue chip

containing 107 gastric cancer tissues, we found that the FTO expression status detected by IHC was significantly and negatively correlated with the patients' OS. Examination of FTO expression by qPCR and western blotting knocking confirmed higher FTO expression in gastric cancer tissues than their adjacent normal tissues as previously reported. We further demonstrated that FTO reinforced malignant phenotypes of gastric cancer cells including cell proliferation, colony formation, migration and invasion *in vitro* and promoted tumor growth in mice by using FTO knockdown and overexpression techniques. Also, high-throughput transcriptome sequencing of the FTO-knocked down and the

control HGC27 cells showed that the differentially expressed genes were significantly enriched in the PI3K/Akt pathway, one of the most frequently activated signaling pathways in human cancer [27, 28]. Enhanced PI3K/Akt signaling in gastric cancer can result from many factors, such as aberrant protein expression, non-coding RNAs, and RNA methylation [21, 29–32], indicating that the pathway plays an important role in gastric cancer development. Thus, by combined use of FTO knockdown and the Akt phosphorylation activator SC79 in HGC27 cells, we confirmed that FTO exerted its promotion roles via the PI3K/Akt pathway. Taken together, increased FTO expression in gastric cancer enhances PI3K/Akt signaling to promote malignant behaviors of the cancer cells and thereby, affects prognosis of the patients.

FTO is an RNA demethylase that can erase methyl groups of RNAs especially in N-6 methyladenosine and influence the turnover, splicing and translation of mRNA molecules. FTO-targeted mRNA molecules are quite different in different types of cells. Exonic splicing of adipogenic regulatory factor RUNX1T1 regulated by FTO is required for adipogenesis [14], while FTO-controlled expression of ASB2 and RARA in acute myeloid leukemia,  $\beta$ -catenin in cervical squamous cell carcinoma, and MZF1 in lung squamous cell cancer cells are necessary for maintaining and promoting malignancy [15–17]. In gastric cancer, the m6A level in the mRNA of ITGB1, an integrin subunit, is modified by FTO, and overexpressed ITGB1 partially reverse FTO knockdown-inhibited migration and invasion [21]. It is likely that FTO-targeted mRNA molecules vary depending on different cells. However, it is possible that FTO targets a variety of mRNA molecules even in a single cell. How these FTO-targeted mRNA molecules synergize each other to promote tumorigenesis remains to be clarified. Although our results demonstrate that FTO has critical roles in gastric cancer development, there were some pitfalls and drawbacks in present study. First, this study sought to investigate whether FTO has clinical significance in gastric cancer as well as how it affects phenotypic features of cells, but the direct RNA targets of FTO as well as the complicated roles of m6A modifications on gastric cancer has not been explained. Further studies should be applied to find the direct targets of FTO by using a series of methods such as m6A-sequencing and RIP-sequencing. At the same time, the specific regulation mechanism of PI3K/Akt signaling pathway by FTO as m6A modifications eraser has not been clarified yet, but this is also an important research direction of our future experiments.

In conclusions, we systemically investigated FTO expression in gastric cancer and its roles in gastric cancer development. The results indicated that FTO expression was enhanced in a gastric cancer tissue chip and the expression status was inversely correlated with the patients' OS, showing that FTO expression is a potent prognostic biomarker.

Manipulation of FTO expression in gastric cancer cells by knockdown and overexpression demonstrated that FTO enhanced the PI3K/Akt signaling to promote the cell proliferation, colonization, and invasion *in vitro* and tumor growth in mice. Our findings suggest that FTO is a promising therapeutic target for gastric cancer.

**Supplementary Information** The online version contains supplementary material available at <https://doi.org/10.1007/s12032-023-01990-2>.

**Acknowledgements** Gratitude should be expressed to the Comprehensive Experiment Center and the Department of Immunology, School of Basic Medical Sciences, Anhui Medical University for giving precious help in this paper.

**Author contributions** All authors contributed to the study conception and design. ZF conceived and designed the study and experiments involved. YZ performed the experiments and analyzed the data. YL provided gastric cancer samples. JY made suggestions on bioinformatics analysis. YZ and JX wrote the manuscript. All authors read, commented and approved the final manuscript.

**Funding** This study was supported by the grants from The National Natural Science Youth Foundation of China (No. 8190102788).

**Data availability** Data supporting the findings of this study are available from the corresponding author upon reasonable request.

## Declarations

**Competing interests** The authors disclose no potential conflicts of interest.

**Ethical approval** The study was conducted in accordance with the Declaration of Helsinki, and approved by the Ethics Committee of Anhui Medical University (20190362). All animal experiments in this study were approved by the Animal Ethics Committee of Anhui Medical University (LLSC20190402).

## References

1. Bray F, Ferlay J, Soerjomataram I, Siegel RL, Torre LA, Jemal A. Global cancer statistics 2018: GLOBOCAN estimates of incidence and mortality worldwide for 36 cancers in 185 countries. *CA Cancer J Clin.* 2018;68(6):394–424.
2. Chen W, Zheng R, Baade PD, Zhang S, Zeng H, Bray F, Jemal A, Yu XQ, He J. Cancer statistics in China, 2015. *CA Cancer J Clin.* 2016;66(2):115–32.
3. Liu D, Lu M, Li J, Yang Z, Feng Q, Zhou M, Zhang Z, Shen L. The patterns and timing of recurrence after curative resection for gastric cancer in China. *World J Surg Oncol.* 2016;14(1):305.
4. Liu X, Zhang D, Lin E, Chen Y, Li W, Chen Y, Sun X, Zhou Z. Preoperative controlling nutritional status (CONUT) score as a predictor of long-term outcome after curative resection followed by adjuvant chemotherapy in stage II–III gastric Cancer. *BMC Cancer.* 2018;18(1):699.
5. Yoon KJ, Ringeling FR, Vissers C, Jacob F, Pokrass M, Jimenez-Cyrus D, Su Y, Kim NS, Zhu Y, Zheng L, Kim S, Wang X, Doré LC, Jin P, Regot S, Zhuang X, Canzar S, He C, Ming GL, Song H. Temporal control of mammalian cortical neurogenesis by m(6) A methylation. *Cell.* 2017;171(4):877–889.e17.

6. Geula S, Moshitch-Moshkovitz S, Dominissini D, Mansour AA, Kol N, Salmon-Divon M, Hershkovitz V, Peer E, Mor N, Manor YS, Ben-Haim MS, Eyal E, Yunger S, Pinto Y, Jaitin DA, Viukov S, Rais Y, Krupalnik V, Chomsky E, Zerbib M, Maza I, Rechavi Y, Massarwa R, Hanna S, Amit I, Levanon EY, Amariglio N, Stern-Ginossar N, Noverstern N, Rechavi G, Hanna JH. Stem cells. m6A mRNA methylation facilitates resolution of naïve pluripotency toward differentiation. *Science*. 2015; 347(6225):1002–1006.
7. Shi H, Zhang X, Weng YL, Lu Z, Liu Y, Lu Z, Li J, Hao P, Zhang Y, Zhang F, Wu Y, Delgado JY, Su Y, Patel MJ, Cao X, Shen B, Huang X, Ming GL, Zhuang X, Song H, He C, Zhou T. m(6)A facilitates hippocampus-dependent learning and memory through YTHDF1. *Nature*. 2018;563(7730):249–53.
8. Weng H, Huang H, Wu H, Qin X, Zhao BS, Dong L, Shi H, Skibbe J, Shen C, Hu C, Sheng Y, Wang Y, Wunderlich M, Zhang B, Dore LC, Su R, Deng X, Ferchen K, Li C, Sun M, Lu Z, Jiang X, Marcucci G, Mulloy JC, Yang J, Qian Z, Wei M, He C, Chen J. METTL14 inhibits hematopoietic stem/progenitor differentiation and promotes leukemogenesis via mRNA m(6)A modification. *Cell Stem Cell*. 2018;22(2):191–205.e9.
9. Du Y, Hou G, Zhang H, Dou J, He J, Guo Y, Li L, Chen R, Wang Y, Deng R, Huang J, Jiang B, Xu M, Cheng J, Chen GQ, Zhao X, Yu J. SUMOylation of the m6A-RNA methyltransferase METTL3 modulates its function. *Nucleic Acids Res*. 2018;46(10):5195–208.
10. Chen M, Wei L, Law CT, Tsang FH, Shen J, Cheng CL, Tsang LH, Ho DW, Chiu DK, Lee JM, Wong CC, Ng IO, Wong CM. RNA N6-methyladenosine methyltransferase-like 3 promotes liver cancer progression through YTHDF2-dependent posttranscriptional silencing of SOCS2. *Hepatology*. 2018;67(6):2254–70.
11. Zhang S, Zhao BS, Zhou A, Lin K, Zheng S, Lu Z, Chen Y, Sulman EP, Xie K, Böglér O, Majumder S, He C, Huang S. m(6)A Demethylase ALKBH5 maintains tumorigenicity of glioblastoma stem-like cells by sustaining FOXM1 Expression and Cell Proliferation Program. *Cancer Cell*. 2017;31(4):591–606.e6.
12. Liu J, Eckert MA, Harada BT, Liu SM, Lu Z, Yu K, Tienda SM, Chryplewicz A, Zhu AC, Yang Y, Huang JT, Chen SM, Xu ZG, Leng XH, Yu XC, Cao J, Zhang Z, Liu J, Lengyel E, He C. m(6)A mRNA methylation regulates AKT activity to promote the proliferation and tumorigenicity of endometrial cancer. *Nat Cell Biol*. 2018;20(9):1074–83.
13. Cui Q, Shi H, Ye P, Li L, Qu Q, Sun G, Sun G, Lu Z, Huang Y, Yang CG, Riggs AD, He C, Shi Y. m(6)A RNA methylation regulates the self-renewal and tumorigenesis of glioblastoma stem cells. *Cell Rep*. 2017;18(11):2622–34.
14. Zhao X, Yang Y, Sun BF, Shi Y, Yang X, Xiao W, Hao YJ, Ping XL, Chen YS, Wang WJ, Jin KX, Wang X, Huang CM, Fu Y, Ge XM, Song SH, Jeong HS, Yanagisawa H, Niu Y, Jia GF, Wu W, Tong WM, Okamoto A, He C, Rendtlew Danielsen JM, Wang XJ, Yang YG. FTO-dependent demethylation of N6-methyladenosine regulates mRNA splicing and is required for adipogenesis. *Cell Res*. 2014;24(12):1403–19.
15. Li Z, Weng H, Su R, Weng X, Zuo Z, Li C, Huang H, Nachtergaele S, Dong L, Hu C, Qin X, Tang L, Wang Y, Hong GM, Huang H, Wang X, Chen P, Gurbuxani S, Arnovitz S, Li Y, Li S, Strong J, Neilly MB, Larson RA, Jiang X, Zhang P, Jin J, He C, Chen J. FTO plays an oncogenic role in acute myeloid leukemia as a N(6)-Methyladenosine RNA demethylase. *Cancer Cell*. 2017;31(1):127–41.
16. Zhou S, Bai ZL, Xia D, Zhao ZJ, Zhao R, Wang YY, Zhe H. FTO regulates the chemo-radiotherapy resistance of cervical squamous cell carcinoma (CSCC) by targeting  $\beta$ -catenin through mRNA demethylation. *Mol Carcinog*. 2018;57(5):590–7.
17. Liu J, Ren D, Du Z, Wang H, Zhang H, Jin Y. m(6)A demethylase FTO facilitates tumor progression in lung squamous cell carcinoma by regulating MZF1 expression. *Biochem Biophys Res Commun*. 2018;502(4):456–64.
18. Xu D, Shao W, Jiang Y, Wang X, Liu Y, Liu X. FTO expression is associated with the occurrence of gastric cancer and prognosis. *Oncol Rep*. 2017;38(4):2285–92.
19. Xu Z, Chen Q, Shu L, Zhang C, Liu W, Wang P. Expression profiles of m6A RNA methylation regulators, PD-L1 and immune infiltrates in gastric cancer. *Front Oncol*. 2022;12:970367.
20. Zhou Y, Wang Q, Deng H, Xu B, Zhou Y, Liu J, Liu Y, Shi Y, Zheng X, Jiang J. N6-methyladenosine demethylase FTO promotes growth and metastasis of gastric cancer via m(6)A modification of caveolin-1 and metabolic regulation of mitochondrial dynamics. *Cell Death Dis*. 2022;13(1):72.
21. Wang D, Qu X, Lu W, Wang Y, Jin Y, Hou K, Yang B, Li C, Qi J, Xiao J, Che X, Liu Y. N(6)-Methyladenosine RNA Demethylase FTO Promotes Gastric Cancer Metastasis by Down-Regulating the m6A Methylation of ITGB1. *Front Oncol*. 2021;11:681280.
22. Yue L, Zhang R, Chen S, Duan G. Risk score prediction model of prognosis in GC patients by age and gender combined with m6A modification genes FTO and RBM15. *Front Cell Dev Biol*. 2022;10:710708.
23. Zhao Y, Yan X, Wang Y, Zhou J, Yu Y. N6-methyladenosine regulators promote malignant progression of gastric adenocarcinoma. *Front Oncol*. 2021;11:726018.
24. Xu X, Zhou E, Zheng J, Zhang C, Zou Y, Lin J, Yu J. Prognostic and predictive value of m6A “Eraser” related gene signature in gastric cancer. *Front Oncol*. 2021;11:631803.
25. Azzam SK, Alsafar H, Sajini AA. FTO m6A demethylase in obesity and cancer: implications and underlying molecular mechanisms. *Int J Mol Sci*. 2022;23(7):3800. <https://doi.org/10.3390/ijms23073800>
26. Chen XY, Zhang J, Zhu JS. The role of m(6)A RNA methylation in human cancer. *Mol Cancer*. 2019;18(1):103.
27. Alzahrani AS. PI3K/Akt/mTOR inhibitors in cancer: at the bench and bedside. *Semin Cancer Biol*. 2019;59:125–32.
28. Wang C, Yang Z, Xu E, Shen X, Wang X, Li Z, Yu H, Chen K, Hu Q, Xia X, Liu S, Guan W. Apolipoprotein C-II induces EMT to promote gastric cancer peritoneal metastasis via PI3K/AKT/mTOR pathway. *Clin Transl Med*. 2021;11(8):e522.
29. Wu S, Chen M, Huang J, Zhang F, Lv Z, Jia Y, Cui YZ, Sun LZ, Wang Y, Tang Y, Verhoeft KR, Li Y, Qin Y, Lin X, Guan XY, Lam KO. ORAI2 promotes gastric cancer tumorigenicity and metastasis through PI3K/Akt signaling and MAPK-dependent focal adhesion disassembly. *Cancer Res*. 2021;81(4):986–1000.
30. Wang L, Bo X, Yi X, Xiao X, Zheng Q, Ma L, Li B. Exosome-transferred LINC01559 promotes the progression of gastric cancer via PI3K/AKT signaling pathway. *Cell Death Dis*. 2020;11(9):723.
31. Huang Y, Zhang J, Hou L, Wang G, Liu H, Zhang R, Chen X, Zhu J. LncRNA AK023391 promotes tumorigenesis and invasion of gastric cancer through activation of the PI3K/Akt signaling pathway. *J Exp Clin Cancer Res*. 2017;36(1):194.
32. Zhang F, Li K, Pan M, Li W, Wu J, Li M, Zhao L, Wang H. miR-589 promotes gastric cancer aggressiveness by a LIFR-PI3K/AKT-c-Jun regulatory feedback loop. *J Exp Clin Cancer Res*. 2018;37(1):152.

**Publisher's Note** Springer Nature remains neutral with regard to jurisdictional claims in published maps and institutional affiliations.

Springer Nature or its licensor (e.g. a society or other partner) holds exclusive rights to this article under a publishing agreement with the author(s) or other rightsholder(s); author self-archiving of the accepted manuscript version of this article is solely governed by the terms of such publishing agreement and applicable law.



## Authors and Affiliations

Yuxuan Zhu<sup>1</sup> · Jing Yang<sup>2</sup> · Yongxiang Li<sup>2</sup> · Jiegou Xu<sup>3</sup> · Zheng Fang<sup>1,2</sup> 

✉ Yongxiang Li  
liyongxiang@ahmu.edu.cn

✉ Jiegou Xu  
xujiegou@ahmu.edu.cn

✉ Zheng Fang  
fangzheng2021@njmu.edu.cn

<sup>2</sup> Department of General Surgery, The First Affiliated Hospital of Anhui Medical University, 218 Jixi Avenue, Hefei 230031, Anhui, China

<sup>3</sup> Department of Immunology, School of Basic Medical Science, Anhui Medical University, Hefei 230032, Anhui, China

<sup>1</sup> Department of Emergency Surgery, The First Affiliated Hospital of Anhui Medical University, 218 Jixi Avenue, Hefei 230031, Anhui, China